PHYSICAL REVIEW B **87**, 094101 (2013)

Relaxor behavior of $Ca_xBa_{1-x}Nb_2O_6$ ($0.18 \leqslant x \leqslant 0.35$) tuned by Ca/Ba ratio and investigated by resonant ultrasound spectroscopy

Chandra Shekhar Pandey* and Jürgen Schreuer
Institute of Geology, Mineralogy and Geophysics (Crystallography), Ruhr University Bochum, Universitaetsstrasse 150, 44801-Bochum, Germany

Manfred Burianek and Manfred Mühlberg
Institute of Crystallography, University of Cologne, Greinstrasse 6, 50939-Cologne, Germany

(Received 31 December 2012; published 1 March 2013)

Dependence of relaxor behavior of incompletely filled tetragonal tungsten bronze uniaxial relaxor ferroelectric calcium barium niobate ($Ca_xBa_{1-x}Nb_2O_6$, CBN-x) on its composition was investigated by varying Ca/Ba ratio ($0.18 \leqslant x \leqslant 0.35$) and studying its thermal and elastic properties. Recently, we have reported the relaxor behavior CBN-28 with the evidence of the existence of the Burns temperature T_B, and the intermediate characteristic temperature T^* [Pandey *et al.*, Phys. Rev. B **84**, 174102 (2011)]. In this work, we show that the dynamics of polar nanoregions (and hence the relaxor behavior) strongly varies with the Ca/Ba ratio. Evidence is found for a more pronounced relaxor behavior with increasing x. The Curie temperature and the Burns temperature are also very sensitive to the composition, whereas the characteristic temperature T^* appears unaffected from the Ca/Ba ratio. The bonding interaction has been explained on the basis of bulk modulus, Poisson's ratio, and deviation from Cauchy relations. Presented results open the perspective to understand the variation of relaxor behavior of CBN-x ($\sim 0.18 \leqslant x \leqslant \sim 0.35$) above Curie temperature.

DOI: 10.1103/PhysRevB.87.094101 PACS number(s): 77.80.−e, 77.80.Jk, 62.20.de, 62.65.+k

I. INTRODUCTION

An understanding as to how the polar nanoregions (PNRs) affect the properties of materials is a subject of great curiosity, challenge, and one of the key parameters of interest to the materials scientists as well as to condensed matter physicists. PNRs observed in relaxor ferroelectrics (hereafter relaxors) are an example of this type of challenge. Relaxor ferroelectrics are solid solutions between a relaxor material and a ferroelectric.[1] Relaxors are mainly characterized by these important features: A diffuse phase transition near Curie temperature T_C, and small-sized ordered PNRs whose first nucleation takes place below the Burns temperature T_B.[2] Upon cooling, PNRs show a growing nature, however, their dynamics slows down.[3–9] The slowing down motion of the dynamic PNRs is due to the initiation of the static nature of PNRs at an intermediate characteristic temperature T^*.[10,11] Relaxors belonging to the partially filled tetragonal tungsten bronze (TTB) family have attracted much interest in the last decades due to their outstanding piezoelectric, dielectric, as well as electro-optic properties.[12,13] The unit cell of the TTB structure contains six big voids: two voids with coordination number CN 12 (type $A1$) with CN 15 (type $A2$), and four small voids with CN 9 (type C).[14] Consequently, the general formula for niobates with TTB structure is $(A1)_2(A2)_4C_4Nb_{10}O_{30}$. The $A1$, $A2$, and C positions can be occupied with different cations of suitable size and charge. It has been shown that the origin of relaxor behavior is due to quenched random electric fields, which are related to the cation distribution on the A site of partially filled TTBs, and promotes the formation of polar nanoregions (PNRs) in the paraelectric phase.[15] Among various known lead-free relaxors, $Sr_xBa_{1-x}Nb_2O_6$ (SBN-x) has attracted much importance mainly due to its photorefractive properties;[16] however, the use of SBN is limited due to its much smaller T_C ($\sim$352 K). Calcium barium niobate $Ca_xBa_{1-x}Nb_2O_6$ (hereafter CBN-x) with $0.20 < x < 0.35$ (Refs. 14 and 17) is isostructural to SBN with TTB structure, and $\sim$200 K higher T_C[18] is a future alternative to SBN. In CBN-x, only five of the six A ($A1$ and $A2$) cation sites of the TTB structure are occupied, leading to some degree of disorder and incommensurate structural modulations. From thorough investigations of thermal expansion and elastic properties of single-crystal CBN-28 up to 1503 K, we have recently reported the evidence of the temperatures T_B and T^*.[18]

It is well known that the PNRs strongly affect the relaxor properties[18] and their presence can be noticed mainly by the elastic properties at T_B (Ref. 19) and by the measurement of thermal strain.[20,21] The goal of this paper is to explore how the growing PNRs change with the variation of Ca composition (i.e., Ca/Ba ratio) and hence on the relaxor behavior of CBN-x. To this end, the thermal expansion and the elastic constants of CBN-18 and CBN-35 single crystals were studied between room temperature and 1503 K employing dilatometry and resonant ultrasound spectroscopy, respectively.

II. EXPERIMENTAL DETAILS

Large, transparent, crack and inclusion free, and nearly colorless CBN-18 and CBN-35 single crystals were grown by the Czochralski method.[17] Rectangular parallelepipeds with edge length in the range 2.1–4.1 mm were cut from each grown single crystal and polished to optical quality. The orientation of the samples was controlled by Laue backscattering and Bragg diffraction techniques. Deviations from ideal orientation were less than 0.2°. Opposite faces were parallel to within ± 1 μm. The calculated geometric density $\rho_g = M/l_1l_2l_3$ (M is the sample mass and l_i are the lengths) matches well with the density obtained by the buoyancy method, confirming the high quality of the samples, particularly in respect to geometrical errors.

TABLE I. Characterization of the investigated CBN-x single crystals. ρ_b density as determined by the buoyancy method, T are the temperatures as described in the text.

Sample name →	CBN-18	CBN-28	CBN-35
Reference	This work	Pandey *et al.* (Ref. 18)	This work
CBN-x melt	$Ca_{0.18}Ba_{0.78}Nb_2O_6$	$Ca_{0.28}Ba_{0.72}Nb_2O_6$	$Ca_{0.35}Ba_{0.65}Nb_2O_6$
CBN-x crystal	$Ca_{0.239}Ba_{0.761}Nb_2O_6$	$Ca_{0.279}Ba_{0.721}Nb_2O_6$	$Ca_{0.307}Ba_{0.693}Nb_2O_6$
$l1^*l2^*l3 \| c$ (mm^3)	3.613* 3.626* 2.183	7.493* 6.407* 7.436	3.207* 2.888* 4.191
ρ_b ($gm.cm^3$)	5.353(2)	5.302(2)	5.290(2)
T_C (K) [T_C (°C)]	~601 (328)	~538 (265)	~493 (220)
T_B (K)	~1200	~1100	~1050
T^* (K)	~800	~800	~800

The phase transition temperature of each CBN-x single crystal was obtained by the aid of a differential scanning calorimeter (DSC 404 F1 Pegasus form NETZSCH®) in He purge gas atmosphere. Curie temperature T_C for investigated samples is given in Table I along with the final sample dimensions. The phase transition temperature of CBN-x was found to be very sensitive to the composition and varies depending on the Ca content in the crystals. With increasing x, T_C decreases. In CBN-x, Ca is only accommodating in the $A1$ site, and we strongly believe that this $A1$ site occupancy affects T_C variation with x.

Thermal expansion measurements in the temperature range 300–1523 K were performed on rectangular parallelepipeds using a commercial inductive gauge dilatometer (DIL 402 C form NETZSCH®) in air. The expansion of the samples was measured while applying the heating/cooling rates of 2 K/min. Each run was repeated at least three times to test the reproducibility of the observed strains. The dilatometer was calibrated using corundum ceramic standards with certified thermal expansion tables. More details about the measurement method can be found elsewhere.[18]

Elastic constants were extracted from the resonance spectrum taken from an innovative method of resonant ultrasound spectroscopy (RUS).[22] Resonance spectra on each sample were collected in the temperature range of 300–1503 K using a high-temperature RUS device built in house.[23] A detailed description of the RUS technique[20] and the measurement method used by us[18] can be found elsewhere. Spectra were recorded in 40-K intervals in air. Examples of typical resonance spectra collected on each sample are shown in Fig. 1. From each sample, at least 80 eigenfrequencies in the range 200–1800 kHz were extracted and used in nonlinear least-squares refinements minimizing the quantity $\chi^2 = \sum_{i=1}^{n} w_i((\omega_i^2)_{\text{calc}} - (\omega_i^2)_{\text{obs}})^2$ for n circular eigenfrequencies ($\omega_i = 2\pi\nu_i$) by adjusting the values of the elastic constants c_{ij}. $(\omega_i)_{\text{calc}}$ is the ith calculated frequency and $(\omega_i)_{\text{obs}}$ is the ith observed one. The w_i are individual weights calculated by assuming an experimental error of ±0.1 kHz for each observed resonance frequency. The ω_i depend on sample orientation, shape, and size as well as on mass density and elastic constants. In each cycle of refinement, the eigenfrequencies of the sample were calculated by solving an eigenproblem, the rank of which equals the number of basis functions used. In order to minimize errors due to truncation effects, and due to the limited precision of floating-point numbers, 6900 normalized Legendre polynomials were used for the expansion of the components of the displacement vector. The convergence of the refinement procedure depends critically on the correct assignment of calculated to observed modes. Therefore, the initial guess values for elastic constants at 1503 K were taken from Ref. 18. After correcting the sample dimensions and density due to thermal expansion effects, the elastic constants at each temperature were successively refined starting at 1503 K. At least four resonance spectra (heating → cooling → heating → cooling) were collected on each sample at elevated temperatures to check the reproducibility of elastic constants. No hysteresis and/or irreversible changes were observed in either sample. Further, the inverse quality factor $Q^{-1} = \text{FWHM}/f$ of selected resonances was derived from their resonance frequency f and their full width at half maximum (FWHM) by fitting an asymmetric Lorentzian split function[24,25] to the individual peaks of the observed resonances.

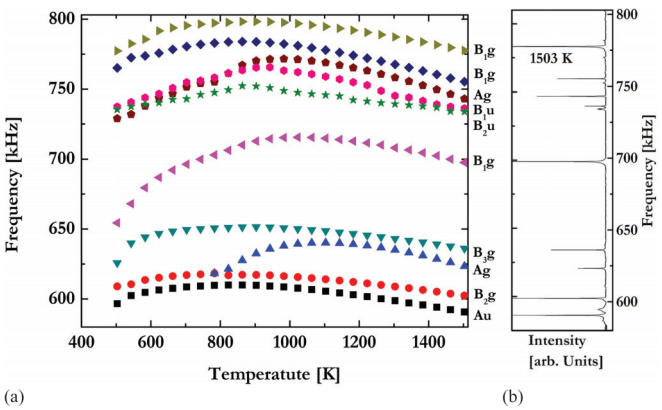

FIG. 1. (Color online) An example of resonance spectrum taken on CBN-35 single crystal: (a) temperature evolution of 10 resonance frequencies; (b) a part of resonance spectrum at 1503 K.

III. RESULTS AND DISCUSSION

A. Thermal expansion

Thermal expansion is a typical anharmonic property of the crystal lattice and is an important factor in crystal growth. Also, it plays an important role in the design and fabrication of devices that exploit their photorefractive or electro-optic properties.[26] The temperature dependence of the elastic constants is usually dominated by anharmonic interaction. As known, a tetragonal TTB structure with point symmetry $4/mmm$ has two independent principal thermal

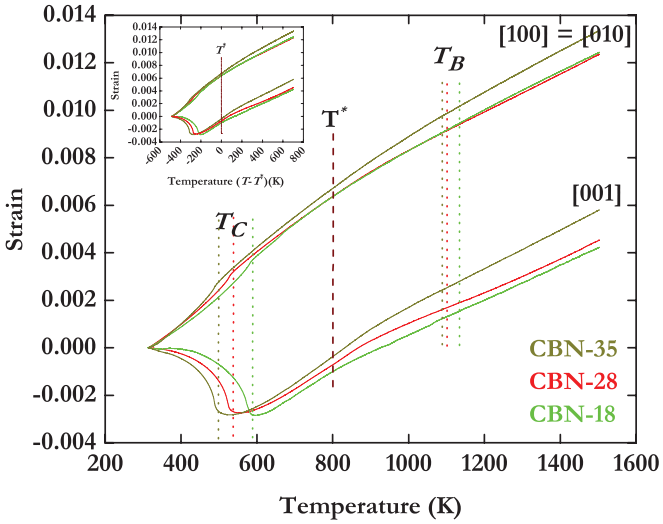

FIG. 2. (Color online) Temperature-induced strains of the CBN-18 and CBN-35, plotted with CBN-28 for the sake of comparison. T-T^* view as shown in inset, showing clearly a deviation from linearity after T^*.

expansion coefficients α_{11} (=α_{22}) and α_{33},[27] which have been derived from temperature-induced strains observed in directions parallel and perpendicular to [001] on each CBN-x sample and is shown in Fig. 2 after calibration correction. The temperature evolution of the strains is anisotropic and highly nonlinear in the investigated temperature range of 300–1523 K. All CBN-x samples show negative thermal expansion (NTE) along [001] between room temperature and T_C. Enormous interests have been shown to the NTE after its discovery by Mary *et al.* in 1996.[28] An explanation for the NTE along [001] in CBN-x single crystals may be given as follows: CBN consists of a network of distorted NbO_6 octahedra linked together in a three-dimensional network by oxygen corners to form three different types of tunnels that connect these octahedra along the [001]. The square channels are occupied by Ca^{2+} ions and the larger pentagonal channels are occupied by Ba^{2+} ions; however, the triangular cross-section channel is empty. The disorder is associated with the NbO_6 octahedra. In the solid solutions of all compositions, the O atoms that join with these two independent octahedra into the chain are disordered. There is a difference in the distances of the one type Nb atom to the upper and lower oxygen atoms along the [001] in the chain. However, other type Nb atoms occupy the general positions, and their distances to all the surrounding O atoms are independent. Hence, due to temperature, octahedra tilting back and forth give rise to thermal contraction. Therefore, the negative thermal expansion along the [001] in CBN-28 may be attributed to the deviation of the Nb site from the center of oxygen coordination octahedra and the disorder in the chains O-Nb-O along [001].[26,29]

In Fig. 2, one can see clearly two distinct deviations from linearity along and perpendicular to [001] with a faint deviation immediately after T_C: (a) for CBN-18 at ∼1200, ∼800, and ∼605 K, (b) for CBN-35 at ∼1050, ∼800, and ∼500 K. In both the samples, the first deviation from linearity at ∼1200 and ∼1050 K corresponds to Burns temperature T_B, where the initiation of PNRs occurs. The second nonlinearity ∼800 K corresponds to T^*, where first dynamic-to-static behavior (due to freezing process initiation) of PNRs occur. Interestingly, it is observed that T^* is independent from Ca/Ba ratio in CBN-x. A more clear view of the invariance of T^* with composition can be seen in the inset of Fig. 2 where strain versus (T-T^*) is plotted. It can be seen that the strain curves progress parallel up until T^*, and after that behavior diverge. For the sake of better understanding the behavior of T_B and T^*, strain curve of CBN-28 is also plotted in this figure. In a research on $Pb(Zn_{1/3}Nb_{2/3})O_3$, T^* is found to be composition dependent.[30] A barely visible third deviation ∼605 and ∼498 K for CBN-18 and CBN-35, respectively, might be hints on T_m. However, a quantitative number for T_m can only be obtained after detailed dielectric investigations. Temperature-induced strains do not show any indication of the occurrence of T_f and hence they depict the occurrence of a diffuse "relaxor-to-ferroelectric" phase transition in CBN-x.

B. Elastic anomalies

The stiffness of the materials against an applied external strain can be best described by its elastic constants and termed as the most fundamental mechanical parameter for crystalline materials. TTB CBN-x single crystals (point symmetry $4/mmm$ in its paraelectric phase) exhibit six symmetry-independent elastic constants (c_{11}, c_{33}, c_{12}, c_{13}, c_{44}, c_{66}).[27] Elastic constants calculated from the observed resonant spectra are graphed in Fig. 3 for both the samples in a relative scale. For the sake of a direct analysis of Ca/Ba ratio on the relaxor properties of CBN-x, the elastic constants of CBN-28 are also plotted with these graphs.

Temperature evolution of all the elastic constants occurs differently, showing their interaction with longitudinal acoustic (LA) and transverse acoustic (TA) waves and a mixture of these. The behavior of longitudinal elastic constants c_{11} of all CBN-x is more or less similar on cooling from higher temperature up to ∼800 K. Below ∼800 K, the deviations from individual behavior is more pronounced, especially in the case for CBN-18 and CBN-35. Comparing the observed deviation at ∼800 K with that of CBN-28 (Ref. 18) gives a clear conclusion about the existence of T^*, and its invariance with the Ca/Ba ratio. On further cooling below T^*, c_{11} of CBN-35 experiences relatively much faster softening than the other two. Considering this softening and correlating it with the recent study on isostructural SBN with composition (small-sized PNRs exist larger in number than the bigger-sized ones with increasing x content),[15] we conclude that the smaller-sized dymanic PNRs are larger in numbers than bigger ones in CBN-35 and still interacting with phonons perpendicular to the polar c axis. A broad conclusion based on the behavior of c_{11} reflects that bigger-size PNRs are present in larger number in CBN-18 than that for CBN-35, and vice versa. Bigger-sized PNRs correlate faster and try to saturate,[18] hence showing relatively less dynamic behavior, as in the case of CBN-18 and CBN-28.

Let us focus on the temperature evolution of longitudinal elastic stiffness c_{33}. On cooling below 1503 K, a first deviation can be seen at ∼1200 K (CBN-18), ∼1100 K (CBN-28), and ∼1050 K (CBN-35), which is a signature of the initiation of PNRs and hence termed as T_B of the individual sample. On

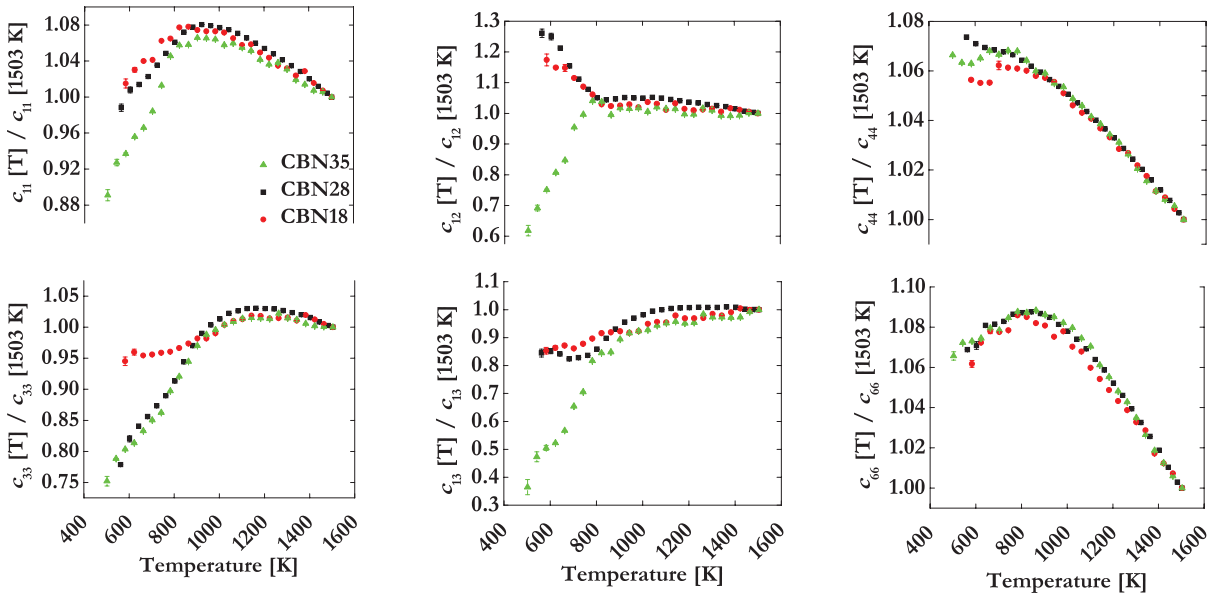

FIG. 3. (Color online) Temperature evolution of the c_{ij} (in relative scale) for CBN-x in its paraelectric phase. The error bars are included for each data point, which are observable only on approaching to the phase transition temperature.

further cooling, c_{33} of all the samples deviates at ~800 K (T^*). A significant softening in c_{33} immediately after T_B can be seen for sample CBN-35, following CBN-28 behavior; however, it is most pronounced among others. This pronounced softening of c_{33} in CBN-35 again confirms the presence of dynamic PNRs in larger number than that for CBN-18, and is related to the growth of dynamic PNRs accompanied by the local strains and their interaction with phonons[31] parallel to the polar c axis. Comparing the physical behavior of c_{33} with c_{11}, we see (Fig. 3) that the signature of T_B in c_{11} seems to be feeble, however, the signature for both T_B and T^* is much more pronounced in c_{33}.

An important difference can be seen in the behavior of the transverse interaction coefficients (TICs) c_{12} and c_{13}. TICs do not control any acoustic waves and are related to the combination of LA and TA waves. Here, we see a completely opposite behavior for CBN-18 and CBN-35. Interestingly, below T^*, c_{12} and c_{13} for CBN-18 follow the stiffening behavior as that for CBN-28. However, for CBN-35, c_{12} and c_{13} show significantly steep softening below T^*. This suggests that the face diagonal reorientational motion of PNRs is more favorable in CBN-35 than that of CBN-18 and CBN-28.[31]

The shear stiffness coefficients c_{44} and c_{66} seem to be independent with the influence of the dynamic PNRs for all the samples. This behavior can be attributed as the fast growing PNRs (static nature) below T_B, whose reorientational motions are suppressed by the shear strain of the TA waves in related directions.[32] The signature of T^* can be seen in c_{44} for all the samples. A further cooling shows a feeble hardening, stating the influence of growing PNRs with more static nature.[18]

An overall softening is significantly higher in the temperature evolution of c_{ij} for CBN-35 compared to others, reflecting that the smaller-sized PNRs are present in larger number (and hence more pronounced relaxor behavior) for the higher value of x in CBN-x and vice versa. Presented results give clear evidence that temperature evolution of the elastic properties and hence the relaxor behavior depends on the Ca/Ba ratio.

We observe that CBN-18 is much softer than CBN-35 (~21% at 1503 K). This high value of stiffness can best be explained by the elastic S value, which allows for a semi-quantitative interpretation of elastic properties of crystals.[33] The elastic S value can be calculated by the formula $S = CM_V = CM_W/(L\rho)$ with the Loschmidt number L, density ρ, and molar weight M_W. C, the mean elastic stiffness can be calculated by $C = (c_{11} + c_{22} + c_{33} + c_{44} + c_{55} + c_{66} + c_{12} + c_{13} + c_{23})/9$, and represents the elasticity to a broader extent. Under the assumption that the interactions between cations and surrounding anions are similar in a compound X and in its stable constituents X_i the S value of X can be decomposed in additive contributions $S(X_i)$ according to $S(X) = \sum S(X_i)$. This quasiadditivity rule holds within 10% for perovskites.[34] Unfortunately, the elastic S value for Nb_2O_5 was not known, instead the problem was solved by first deriving values of S(CBN-28) from its elastic constants[18] and then using the relation $0.28S(CaO) + 0.72S(BaO) + S(Nb_2O_5) = S$(CBN-28). The calculated S value was found to be 1300, 1403, and 1422 for CBN-18, CBN-28, and CBN-35, respectively, at 1503 K. It is known that S values of CaO (338) are higher than the S value of SrO (311);[34] it was quite obvious that CBN-35 (because of the high value of Ca compared to CBN-18) exhibits a higher value of elastic stiffness than CBN-18. Similarly, the Ca content in CBN-35 is slightly higher than that for CBN-28, and hence CBN-35 exhibits slightly higher elastic stiffnesses than those of CBN-28.

Considering interatomic bonding, phonon-related properties, e.g., Poisson's ratio and bulk modulus, are the most important parameters. Isotropic bulk (B) and shear (G) modulus can be calculated from the calculated elastic constants using the average of the Voigt and Reuss approximations[35] best known as Voigt-Reuss-Hill (VRH).[36] Isotropic bulk modulus

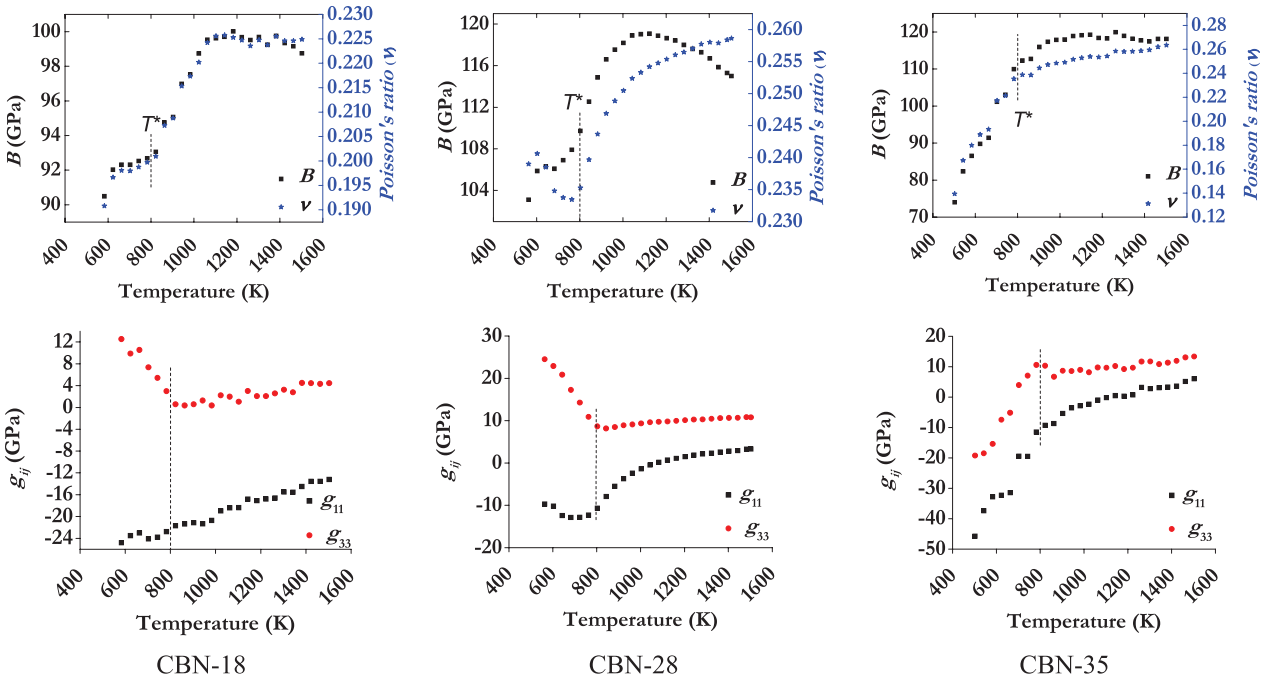

FIG. 4. (Color online) Temperature evolutions of the isotropic bulk modulus (B), Poisson's ratio (ν) above T_C. Deviations from Cauchy relations (g_{ij}) are also plotted, showing a considerable difference in the values of B and g_{ij}.

for CBN-x is shown in Fig. 4 as a function of temperature. A softening of bulk modulus below T_B was observed for all the samples. A decreasing trend of the bulk modulus below T_B confirms the formation of nanoregions in the highly localized deformation regions,[37] and the material is approaching phase transition.[38] Smallest B of CBN-35, among others, states the strong covalent nature of the solid near T_C.[39]

The Poisson's ratio ν which gives information about the stability against shear strain was calculated using the relation $\nu = 3B - 2G/2(3B + G)$. Poisson's ratio for most known materials falls in the range of 0.25–0.35.[39] A low Poisson's ratio reflects a high ratio of bond-bending stiffness to bond-stretching stiffness. The temperature evolution of the Poisson's ratio for CBN-x single crystals is also plotted in Fig. 4. Above T_B, the ν values of CBN-x single crystals are temperature invariant ($\Delta \sim 0.01$), which is more a characteristic of covalent bonding.[40] Below T_B on approaching to T^*, the low values of ν further indicate that the interatomic forces in the crystals are strongly noncentral. Materials with high ν resist compression in favor of shear, however, with small ν materials are easily compressed than sheared.[41] The decreasing trend of ν below T^* for CBN-35 states that its compression strength is small as compared to shear strength relative to other CBN-x, and smallest near T_C among them. The Poisson's ratio value at 1503 K (for CBN-x) is much below 0.5, giving a clear signature that CBN-x is not showing any decomposition or melting behavior.[42]

A more clear picture about the bonding interaction can be best analyzed by the deviation from Cauchy relations (g_{ij}) (Ref. 18) represented by the second-rank tensor invariant $\{g_{ij}\}$, and its temperature evolution is shown in Fig. 4. In all the CBN-x, the behavior of g_{ij} deviates from its normal path, giving a clear indication of the presence of the characteristic temperature T^*. Below $\sim T^*$, the g_{11} for all the samples shows a negative behavior, stating that the directional bonding (covalent) contribution is preferential over nondirectional (Coulomb interaction) contribution, parallel to fourfold axis. A positive trend of g_{33} below T^* in CBN-18 and CBN-28 confirms that the nondirectional bonding contribution is preferential within the (001) plane, however, for CBN-35 a negative trend of g_{33} below T^* states that directional bonding contribution is more preferential within (001). Interestingly, both g_{ij} in CBN-18 follow CBN-28 behavior with two different bonding interactions in solids, however, CBN-35 shows that the covalent bonding contribution is important in all the directions when approaching to T_C. The above said statements can further be strengthened by comparing the values of B and g_{ij} below $\sim T^*$. A large difference ($\sim$ more than 93 GPa) in the values of B and g_{ij} below $\sim T^*$ is for CBN-35 among others; it strongly supports that the directional bonding contribution is in the form of covalent bonding in all directions when approaching to T_C, while it is relatively less favorable for CBN-18 and CBN-28 with a difference of $\sim$78 and $\sim$79 GPa, respectively. It is well known that Coulomb interaction favors the ferroelectric state.[43] A closure examination of the g_{33} behavior for CBN-18 and CBN-28 shows that the preferential bonding interaction is Coulomb type[34] and hence depicts relatively less relaxor behavior; however, in the case of CBN-35, the bonding interaction is still of covalent type, favoring stronger relaxor behavior among others.

The energy loss (or dissipation) is related to the quality factor Q of the resonance. Temperature evolution of the inverse quality factors (Q^{-1}) of the observed resonance modes (taken from Fig. 1) is shown in Fig. 5. Above T^* up until 1503 K, small values of Q^{-1} state that the peaks of the observed resonances are sharp and there is no signature of energy losses. However,

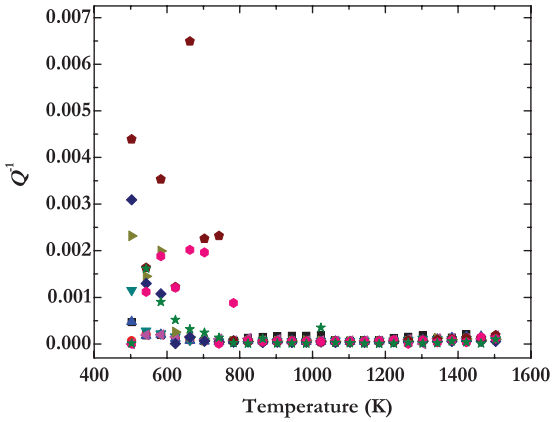

FIG. 5. (Color online) Temperature evolution of inverse quality factor of the resonance modes (taken from Fig. 1).

the dissipation of the peaks starts below T^* which further gives an indication of the partial static nature of the PNRs. Observed resonance modes show an attenuation of the one resonance mode (green star) at ∼1050 K is likely to be associated with the origin of PNRs. Further, large Q^{-1} of all the resonance modes at ∼800 K gives a clear hint of the first switching of dynamic PNRs in static. Some of the modes which are mainly driven by TA (mainly c_{44}) waves are still available in the ferroelectric phase below T_C. However, modes which are mainly driven by LA waves (mainly c_{33}) and still having small PNRs strongly fluctuate in the vicinity of phase transitions and therefore disappear below T_C. The observed modes below T_C seem to be unaffected by the mechanical interactions during phase transitions due to the fast growing nature of PNRs.

Due to strong anisotropic ultrasound attenuation and the growing influence of the quasistatic-to-static PNRs below T_C, it was not possible to get enough resonances and hence reliable elastic constants in the ferroelectric phase.

IV. CONCLUSIONS

Systematic studies of the relaxor behavior of CBN-x single crystals have been studied using resonant ultrasound spectroscopy. A clear evidence of relaxor behavior dependence on the Ca/Ba ratio was observed. Major conclusions include (i) the higher value of x in CBN-x reflects more pronounced relaxor behavior, and vice versa, and (ii) T^* is independent of composition; however, T_B varies. It is interesting that PNRs initiate a local phase transition at T^*,[44] however, to get its complete atomistic picture is still a challenge. Presented results help to explain the dynamic behavior of PNRs considering elastic properties of the relaxor CBN-x below T_B. Negative thermal expansion below room temperature has been explained on crystal-structure basis. The bonding interaction has been explained on the basis of bulk modulus, Poisson's ratio, and deviation from Cauchy relations. When approaching to T_C, preferential directional bonding contributions in the form of "covalent bonding" in all direction of CBN-35 were observed. However, in the case of CBN-18 and CBN-28, the bonding contribution is found to be directionally dependent.

*chandrashekhar.pandey@rub.de

[1] R. E. Cohen, Nature (London) **441**, 941 (2006).
[2] G. Burns and F. H. Dacol, Phys. Rev. B **28**, 2527 (1983); Solid State Commun. **48**, 853 (1983).
[3] G. Xu, J. Wen, C. Stock, and P. M. Gehring, Nat. Mater. **7**, 562 (2008).
[4] I.-K. Jeong, T. W. Darling, J. K. Lee, Th. Proffen, and R. H. Heffner, Phys. Rev. Lett. **94**, 147602 (2005), and references therein.
[5] P. M. Gehring, S. Wakimoto, Z.-G. Ye, and G. Shirane, Phys. Rev. Lett. **87**, 277601 (2001).
[6] S. Wakimoto *et al.*, Phys. Rev. B **65**, 172105 (2002).
[7] R. Blinc, V. Laguta, and B. Zalar, Phys. Rev. Lett. **91**, 247601 (2003).
[8] G. Xu, G. Shirane, J. R. D. Copley, and P. M. Gehring, Phys. Rev. B **69**, 064112 (2004).
[9] P. M. Gehring, H. Hiraka, C. Stock, S.-H. Lee, W. Chen, Z.-G. Ye, S. B. Vakhrushev, and Z. Chowdhuri, Phys. Rev. B **79**, 224109 (2009).
[10] D. La-Orauttapong, J. Toulouse, J. L. Robertson, and Z.-G. Ye, Phys. Rev. B **64**, 212101 (2001).
[11] D. La-Orauttapong, J. Toulouse, Z.-G. Ye, W. Chen, R. Erwin, and J. L. Robertson, Phys. Rev. B **67**, 134110 (2003).
[12] L. E. Cross, Ferroelectrics **76**, 241 (1987).
[13] Y. Xu, *Ferroelectric Materials and Their Applications* (North-Holland, Amsterdam 1991).
[14] M. Eßer, M. Burianek, D. Klimm, and M. Mühlberg, J. Cryst. Growth **240**, 1 (2002).
[15] V. Shvartsman, W. Kleemann, T. Lukasiewicz, and J. Dec, Phys. Rev. B **77**, 054105 (2008), and references therein.
[16] F. Kahmann, J. Höhne, R. Pankrath, and R. A. Rupp, Phys. Rev. B **50**, 2474 (1994).
[17] M. Burianek, B. Joschko, I. Kerkamm, T. Schoenbeck, D. Klimm, and M. Mühlberg, J. Cryst. Growth **299**, 413 (2007); B. Joschko, Ph.D. thesis, University of Cologne, 2007.
[18] C. S. Pandey, J. Schreuer, M. Burianek, and M. Mühlberg, Phys. Rev. B **84**, 174102 (2011).
[19] S. D. Prokhorova and S. G. Lushnikov, Ferroelectrics **90**, 187 (1989).
[20] A. S. Bhalla, R. Guo, L. E. Cross, G. Burns, F. H. Dacol, and Ratnakar R. Neurgaonkar, Phys. Rev. B **36**, 2030 (1987).
[21] J. J. De. Yoreo, R. O. Pohl, and G. Burns, Phys. Rev. B **32**, 5780 (1985).
[22] A. Migliori and J. Sarrao, *Resonant Ultrasound Spectroscopy* (Wiley, New York, 1997); A. Migliori, J. L. Sarrao, W. M. Visscher, T. M. Bell, Ming Lei, Z. Fisk, and R. G. Leisure, Phys. B(Amsterdam) **183**, 1 (1993).
[23] C. S. Pandey, Ph.D. thesis, Ruhr University Bochum, 2010.
[24] J. Schreuer, C. Thybaut, M. Prestat, J. Stade, and E. Haussuhl, in *Proceedings of the IEEE Symposium on Ultrasonics*, Vol. 1 (IEEE, New York, 2003), pp. 196–199.
[25] J. Schreuer and C. Thybaut, in *Proceedings of the IEEE Ultrasonics Symposium*, Vol. 1 (IEEE, New York, 2005), pp. 695–698.
[26] A. Gazarella, T. Wieting, and D. H. Wu, J. Appl. Phys. **98**, 043113 (2005).

[27]J. F. Nye, *Physical Properties of Crystals* (Clarendon, Oxford, 1987).
[28]T. A. Mary, J. S. Evans, O. Vogt, and A. W. Sleight, Science **272**, 90 (1996).
[29]J. Li, A. Yokochi, T. G. Amos, and A. W. Sleight, Chem. Mater. **14**, 2602 (2002).
[30]M. Roth, E. Mojaev, E. Dul'kin, P. Gemeiner, and B. Dkhil, Phys. Rev. Lett. **98**, 265701 (2007).
[31]O. Svitelskiy, A. V. Suslov, J. B. Betts, A. Migliori, G. Yong, and L. A. Boatner, Phys. Rev. B, **78**, 064113 (2008).
[32]J-H Ko, S. G. Lushnikov, D. H. Kim, S. Kojima, B.-E. Jun, and Y. H. Hwang, J. Appl. Phys. **104**, 104105 (2008).
[33]S. Haussühl, Z. Kristallogr. **205**, 215 (1993).
[34]J. Schreuer, and S. Haussühl, EMU Notes Mineralogy **7**, 173 (2005).
[35]O. L. Anderson, *Physical Acoustics*, Vol. III (Academic, New York, 1965).
[36]D. H. Chung and W. R. Buessem, J. Appl. Phys. **38**, 2535 (1967).
[37]Y. L. Hao, S. J. Li, B. B. Sun, M. L. Sui, and R. Yang, Phys. Rev. Lett. **98**, 216405 (2007).
[38]L. Dong, D. S. Stone, and R. S. Lakes, Philos. Mag. Lett. **90**, 23 (2010).
[39]G. N. Greaves, A. L. Greer,, A. L. Greer, R. S. Lakes, and T. Rouxel, Nat. Mater. **10**, 823 (2011).
[40]Y. Suzuki, V. R. Fanelli, J. B. Betts, F. J. Freibert, C. H. Mielke, J. N. Mitchell, M. Ramos, T. A. Saleh, and A. Migliori, Phys. Rev. B **84**, 064105 (2011).
[41]T. Rouxel, H. Ji, J. P. Guin, F. Augereau, and B. Rufflé, J. Appl. Phys. **107**, 094903 (2010).
[42]W. Köster and H. Franz, Metall. Rev. **6**, 1 (1961).
[43]R. E. Cohen, Nature (London) **358**, 136 (1992).
[44]B. Dkhil, P. Gemeiner, A. Al-Barakaty, L. Bellaiche, E. Dul'kin, E. Mojaev, and M. Roth, Phys. Rev. B **80**, 064103 (2009).